

Lab on a Chip

Accepted Manuscript



This is an *Accepted Manuscript*, which has been through the Royal Society of Chemistry peer review process and has been accepted for publication.

Accepted Manuscripts are published online shortly after acceptance, before technical editing, formatting and proof reading. Using this free service, authors can make their results available to the community, in citable form, before we publish the edited article. We will replace this *Accepted Manuscript* with the edited and formatted *Advance Article* as soon as it is available.

You can find more information about *Accepted Manuscripts* in the [Information for Authors](#).

Please note that technical editing may introduce minor changes to the text and/or graphics, which may alter content. The journal's standard [Terms & Conditions](#) and the [Ethical guidelines](#) still apply. In no event shall the Royal Society of Chemistry be held responsible for any errors or omissions in this *Accepted Manuscript* or any consequences arising from the use of any information it contains.



Journal Name

ARTICLE

A programmable microfluidic static droplet array for droplet generation, transportation, fusion, storage, and retrieval

Si Hyung Jin,^{‡a} Heon-Ho Jeong,^{‡a} Byung Jin Lee,^a Sung-Sik Lee,^b and Chang-Soo Lee^{*a}

Received 00th January 20xx,
Accepted 00th January 20xx

DOI: 10.1039/x0xx00000x

www.rsc.org/

We present a programmable microfluidic static droplet array (SDA) device that can perform user-defined multistep combinatorial protocols. It combines the passive storage of aqueous droplets without any external control with integrated microvalves for discrete sample dispensing and dispersion-free unit operation. The addressable picoliter-volume reaction is systematically achieved by consecutively merging programmable sequences of reagent droplets. The SDA device is remarkably reusable, able to perform identical enzyme kinetics experiments at least 30 times via the automated cross-contamination-free removal of droplets from the individual hydrodynamic traps. Taken together, this programmable and reusable universal SDA device will be a general microfluidic platform that can be reprogrammed for multiple applications.

1. Introduction

The technology of handling droplets in microfluidics has advanced over the past decade.^{1–11} By the integration of microvalves in closed channels or embedding an electrode array for controlling the electrostatic force, we can precisely handle liquid droplets in space and time.^{12–18} The fully integrated microfluidic device is able to perform a tremendous number of reactions in parallel or simultaneously and promises wide application from fundamental biology to single-cell analysis.^{19–24} The microvalve-based microfluidics shows the benefit of the scaling of dimensions to precisely generate picoliters (pL) volume droplets and enable the rapid mixing of reagents in the small droplets, leading to reduced reagent consumption and reaction time.^{12–14, 34, 35} These capabilities have made it an attractive platform for high-throughput screening and high-content screening applications, whereas the programmable manipulation of nanoliter (nL) volume droplets using electrostatic forces has received great attention as a promising platform for sample preparation or processing automation in diagnostics.^{15–18, 20, 22, 24}

Despite the advances in microfluidic devices, there is no universal platform that would be ideal for users to perform any experiment on demand. It is technically limited to integrating all specific fluid handling techniques, a customized design for each application, or changes in protocol. Consequently, at this moment, the users have to wait until a developer completes iterative cycles of device design,

fabrication, and evaluation, which is a major obstacle to the development of new applications and limits user flexibility and community access. In considering how programmable integrated electronic circuits foster the creation of a broader community of developers and non-expert users, the advancement of programmable microfluidic devices stands to dramatically enhance the popularity and impact of microfluidic systems.²⁵

Here, we propose a microfluidic static droplet array (SDA) device that accomplishes all basic functions of unit operations such as generation, transportation, immobilization, fusion, storage, observation, and retrieval within a parallel series of droplets in a single integrated device. The methodology presented here executes the groundwork for a highly parallel droplet array. The principle of SDA design relies on hydrodynamic trapping: fluidic resistance along the straight channel is smaller, so the droplets in the flow are carried into the hydrodynamic trap, but once the traps are filled, the flow is redirected to the bypass channels.^{26–33} Although previous studies demonstrated fundamental principle of hydrodynamic trapping in the microfluidic devices, they are still limited in formation of combinatorial droplet array containing different chemical species or mixture of chemical species in a droplet. Unlike previous results, our SDA device is designed to control the size and number of droplets immobilized in the hydrodynamic trap. The capability of programmable operation produces a combinatorial droplet array consisting of various elements by a sequentially repetition of droplet merging, storage, and mixing. This entire procedure is accomplished within a few minutes. The programmability and addressability result in performance comparable to that of a conventional microtiter plate system due to the full automatic procedure on demand.

Furthermore, we can retrieve trapped droplets from the SDA by switching the trap and fluctuation valve. This retrieval

^aDepartment of Chemical Engineering, Chungnam National University, Daejeon, Republic of Korea.

E-mail: rhadum@cnu.ac.kr

^bInstitute of Biochemistry, Department of Biology, ETH Zürich, Zürich, Switzerland.

† Electronic Supplementary Information (ESI) available: Fig. S1 to S5 and Movie S1. See DOI: 10.1039/x0xx00000x

‡ These authors contributed equally.

provides a new opportunity to reproduce several experiments in a single device, overcoming the drawback of the conventional approach that requires disposal of the device after every experiment. As a demonstration, we repeatedly performed an enzyme kinetic assay more than 30 times with a single device. The reusability of this SDA integrated with the microvalve technique dramatically reduces the number of complicated connections to external control fluidics, greatly simplifying preparation and operation. Consequently, our SDA device can be easily implemented with conventional and soft lithography methods. The combination of hydrodynamics and the microvalve technique allows us to eliminate the shortcomings of each method; the hydrodynamic approach allows the simultaneous manipulation of a large number of droplets, whereas the microvalve technique for retrieval gives dexterity in reusability, addressability, and combinatorial throughput.

2. Experimental methods

2.1. Chemicals and reagents

As continuous phases, we used mineral oil and SPAN-80 (Sigma-Aldrich, MI, USA) in the demonstration of SDA device functionality and FC-40 oil and 1*H*,1*H*,2*H*,2*H*-Perfluoro-1-octanol (Sigma-Aldrich, MI, USA) in the enzyme reaction experiment. We visualized the liquid by the addition of red (Alexa Flour-568, Life Technology, CA, USA) and green fluorescent dyes (NaFl, MI, Sigma-Aldrich). Yeast cell suspended solution (YPD medium, $OD_{600} \approx 0.1$) was used for visualizing the vortex flow in droplet. Fluorescein di(β -D-galactopyranoside) (FDG) and β -galactosidase (β -gal) were purchased from Sigma-Aldrich (MI, USA) for visualizing the enzyme reaction.

2.2. Microfluidic device fabrication

We fabricated the SDA microfluidic device by conventional multi-layer soft lithography with microfabricated wafers and poly(dimethylsiloxane) (PDMS, Sylgard 184, Dow Corning, MI, USA).³⁰ The device consists of a PDMS fluidic layer and a pneumatic control layer. The wafer mold for the fluidic layer was fabricated by both a negative photoresist (SU-8 3025, Microchem, MA, USA) and a positive photoresist (AZ9260 and AZ400K, respectively, AZ Electronic Materials, Luxembourg). A rectangular channel of 15 μm height and a round channel of 15 μm height for the microvalve were patterned by the negative and positive photoresists, respectively. Afterward, PDMS (Sylgard 184, 10:1 mixing ratio of elastomer and cross-linker) was poured into the fluidic mold and cured in a 65 °C oven for 1 hour. It was later peeled off from the fluidic mold, and holes were introduced at the end of the channels. For the bottom control layer, a 25 μm layer of PDMS (Sylgard 184, 20:1 mixing ratio of elastomer and cross-linker) was coated on the control mold by spin coating (rpm = 2500), and it was heated for 45 min at 65°C in an oven. Finally, the upper fluidic layer was aligned on the PDMS-coated control mold and incubated in a 65 °C oven for 12 hours. Then, the attached PDMS was peeled

off from the control mold, and holes for the tubing were introduced at the end of the PDMS channels and bonded to a glass slide by oxygen plasma treatment.

2.3. Device operation

We automatically control the opening and closing of the microchannel and microvalves by applying positive pressure and negative pressure, respectively. Nitrogen gas and an air compressor (GAST P104-AA, IDEX corporation, USA) were connected to 24 solenoid valves that were connected to a relay board (Stanford Microfluidic Foundry, USA).^{34, 35} The relay board was controlled by a USB I/O 24 R module (Elexol, Australia) via a LabVIEW (National Instruments Co., TX, USA) based software. The schematic of the whole system is presented in Fig. S1†. The SDA device was mounted onto an inverted microscope (TE-2000U, Nikon, Japan). Images were captured by a CCD camera (Coolsnap cf, Photometrics, AZ, USA) or a high-speed camera (Phantom Miro EX2, Vision research, NJ, USA) and analyzed by image analysis software (Image Pro, Media Cybernetics, MD, USA). We note that the systems could eventually be fully automated being that all operating components including the microfluidics, syringe pumps, and microscopy are controlled by a computer.

3. Results and Discussion

3.1. Basic design of the static droplet array (SDA)

The basic concept of the SDA is designed to follow the previously reported mechanism of hydrodynamic trapping.²⁶⁻³³ There are two main streams toward the straight and bypass channels in the SDA. When a hydrodynamic trap is empty, the straight channel has a lower flow resistance than that of the bypass channel. As a result, the fluid naturally flows along the straight channel. A droplet in the flow is carried by this main stream into the hydrodynamic trap. This droplet immobilized in the hydrodynamic trap acts as a plug, rapidly increasing the flow resistance along the straight channel and redirecting the main flow to the bypass channel. The subsequent droplets will then be carried along the bypass channel and be immobilized into the next hydrodynamic trap in series. The SDA will be designed in the form of a miniature conventional microwell plate. The static droplet array (SDA) device consists of a droplet generator and a drop array (Fig. 1). Droplets are individually generated by a computer-controlled microvalve and immobilized into multiple hydrodynamic traps in an orderly manner. (Fig. 1B, right). On top of this SDA, another microvalve controls the volume, composition, formation cycle and sequence of the droplets (Fig. 1B, left).

3.2. Droplet generation on demand

We generated aqueous reagent droplets in an immiscible continuous oil phase. Prior to generating the droplets, the whole microfluidic channel in the SDA device is filled with oil to wet the surface, and aqueous reagents are loaded into reagent channels that are perpendicularly oriented to the oil channel

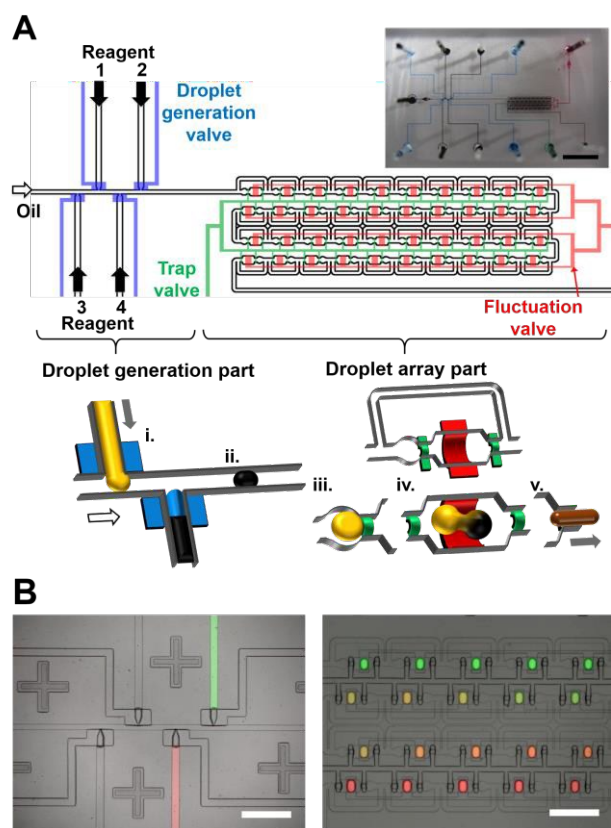


Fig. 1 Design of a programmable static droplet array (SDA) integrated with microvalves and a hydrodynamic trap array. (A) Schematic diagram for a fully integrated SDA device. The black colored line indicates the microfluidic channels, and the blue, green, and red colored lines are the valves of droplet generation, trap and fluctuation, respectively. SDA accomplishes various functions of unit operations such as (i) generation, (ii) transportation, (iii) immobilization, (iv) fusion and storage, and (v) retrieval. The inset shows optical images of the SDA device. For clear visualization, food dye solutions are injected into the microchannels and microvalves. The actual size of a SDA device containing 40 hydrodynamic traps is approximately 2.4 cm in width and 1.8 cm in length. Scale bar, 3 mm. (B) Overlaid fluorescence and bright field images of droplet generation and droplet array parts. Droplet generation part (left) has four sets of reagent channels and corresponding droplet generation valves. Droplet array part (right) consists of hydrodynamic traps with trap and fluctuation valves. The right image is an example of a droplet array with various concentrations created by controlling addressable valves. Scale bar, 400 μm .

(Fig. 1A and B). The droplet generation valve controls the flow of the reagent right under the junction. When the droplet generation valve is opened, the aqueous reagent flows from the reagent channel into the oil channel. As a result, the reagent is surrounded by oil (Fig. S3A[†]). When the droplet generation valve is closed, the flow of reagent is physically blocked, and then the droplets are created through the interaction between the viscosity and shear stress.^{14, 30, 36-38} In this study, we used mineral oil with the surfactant SPAN80 at a 0.1% concentration as the continuous phase. We generated a specific number of droplets of a precise size on-demand by temporally controlling the opening and closing of the microvalve (Fig. S3A[†]). Upon increasing the duration of the opening of the droplet generation valve, the volume of the reagent droplets increases accordingly (Fig. S3B[†]). For example, the volume of the droplets ranges from 17 pL to 82

pL when the valve is opened for between 30 ms and 100 ms under the hydrostatic pressures of 0.15 MPa for the oil phase and 0.18 MPa for the reagents. Additionally, using the programmed individual actuation of the four droplet generation valves, we can precisely manipulate the distance between adjacent droplets and the order of the droplets created on demand.

3.3. Hydrodynamic trapping

The main purpose of the hydrodynamic trap in series is to create a droplet array for the high-density immobilization of droplets. A hydrodynamic trap consists of four structures: a “microwell” as the trapping site of the droplet, a “capillary path” (controllable narrow channel) formed by the partial closing of the trap valve, a “reaction chamber” for storing and merging the trapped droplet, and a “bypass channel” vertically connected to the entrance of the microwell and the exit of the reaction chamber (Fig. S2[†]). The main function of capillary path is to control the flow of fluids within the microchannel and efficiently trap a droplet in the microwell. In this design, one notable advance is formation of a capillary path in the hydrodynamic trap using the simple operation of microvalve actuation because the capillary path is an important parameter for stabilizing the immobilized droplet in the trap.

The SDA follows the principle of hydrodynamic trapping based on the competition of fluidic resistances in the microstructures of the hydrodynamic trap. The immobilization of the droplets on a specific region (microwell) is caused by the hydrodynamic pressure drop due to the structure of the hydrodynamic trap, and the induced capillary path of the microstructure results from the microvalving action. This passive trapping mechanism is robust and insensitive to fluctuations caused by occasional gas bubbles introduced during the switching of solutions. It is also extremely efficient and thus highly suitable for handling small samples.

The pressure drop in a hydrodynamic trap can be derived by applying the Darcy-Weisbach equation, as previously reported.^{26, 28} The expression is given by

$$\Delta P_{\text{hydraulic}} = \frac{fL\rho L^2}{2D} = \frac{c(\alpha)}{32} \cdot \frac{\mu L Q R^2}{A^3} \quad (1)$$

$$c(\alpha) = f \cdot Re = 96(1 - 1.3553\alpha + 1.947\alpha^2 - 1.7012\alpha^3 + 0.9534\alpha^4 - 0.2537\alpha^5) \quad (2)$$

where $P_{\text{hydraulic}}$ indicates the hydraulic pressure drop and ρ the density of the fluid; f is a correction factor; V is the average flow rate of the fluid; μ is the viscosity of the fluid; and R , Q , and A are the perimeter of the channel, the volumetric flow rate, and the cross-section of the channel, respectively. Re indicates the Reynolds number, and α is the aspect ratio of the channel dimensions in the cross-sectional view. $C(\alpha)$ is the Darcy friction factor multiplied by the Reynolds number.

A simplified diagram of a hydrodynamic trap is shown in Fig. 2A. The hydrodynamic trap is composed of complicated structures such as a microwell, capillary path, reaction chamber and bypass channel. The correlation of the pressure drops across each structure can be expressed as follows:

$$\Delta P_{\text{hydraulic}} = \Delta P_{\text{bypass}} = \Delta P_{\text{microwell}} + 2 \cdot \Delta P_{\text{capillary path}} + \Delta P_{\text{reaction chamber}} \quad (3)$$

The variables of the bypass channel are represented by a subscript b , and the variables of the microwell, capillary path, and reaction chamber are referred to using m , c , and r , respectively. With Expression (1) substituted into Expression (3), the formula is as follows:

$$Q_1 \left(\frac{C(\alpha_m) \mu L_m R_m^2}{32A_m^3} + \frac{2C(\alpha_c) \mu L_c R_c^2}{32A_c^3} + \frac{C(\alpha_r) \mu L_r R_r^2}{32A_r^3} \right) = Q_2 \left(\frac{C(\alpha_b) \mu L_b R_b^2}{32A_b^3} \right) \quad (4)$$

$$\frac{Q_1}{Q_2} = \frac{C(\alpha_b) L_b (W_b + H_f)^2}{C(\alpha_m) L_m (W_m + H_f)^2 \left(\frac{W_b}{W_m} \right)^3 + 2C(\alpha_c) L_c (W_c + H_f)^2 \left(\frac{W_b}{W_c} \right)^3 + C(\alpha_r) L_r (W_r + H_f)^2 \left(\frac{W_b}{W_r} \right)^3} \quad (5)$$

where Q_1 and Q_2 represent the routes of the fluid in the horizontal and vertical directions, respectively. f indicates the fluidic layer, and $C(\alpha)$ is a function that changes depending on the aspect ratio. L , W , and H represent the channel length, width, and height, respectively.

The fluid at the entrance of hydrodynamic trap is divided into horizontal and vertical flows. The volumetric flow rate of fluids (Q_1) sequentially running into the microwell, capillary path, and reaction chamber in the horizontal direction, and the volumetric flow rate of fluids (Q_2) travelling along the bypass channel in the vertical direction are defined, as shown in Fig. 2A and B.

When there is no droplet in microwell, the main flux goes through Q_1 because of the lower hydrodynamic resistance in horizontal direction. Under the condition, a droplet arrives at microwell and is trapped: the hydrodynamic resistance of the trap in horizontal direction increases. As a result, Q_2 is higher than Q_1 and the other droplets go through Q_2 because the bypass channel in vertical direction has a lower hydrodynamic resistance (Fig. 2C).

3.4. Sequential loading and merging of droplets

The fully integrated SDA is designed to immobilize 40 droplets. We could then address the droplets individually because they are sequentially immobilized in hydrodynamic traps. This addressable droplet immobilization technique is conducted in a passive manner; our SDA does not require any additional control to immobilize droplets (see process 1 in Movie S1, ES1†). We demonstrate the individual addressability of the droplet array and the ease of the SDA operation. The droplets are arrayed, and we subsequently generate droplets to load the device as a combinatorial droplet array. This entire procedure is accomplished within a few minutes.

After the first droplet is trapped in a microwell, consider what happens when the following droplet enters the array (Fig. 2C). If the first droplet plugs the microwell, all of the flow is directed toward the bypass channel ($Q_1/Q_2 \approx 0.02$, in the case of Fig. 2C). Otherwise, a second droplet would also enter the microwell. Explained another way, the trapping mode ($Q_1/Q_2 \approx 1.11$) continues until the microwell (55 pL) is fully filled. This provides us with another advance in this developing droplet array, in that we can control the number of droplets that are trapped in one microwell by a simple change of the volume of the droplets created in the droplet generation step (see Fig. S4†).

As shown in Fig. 2C, in the case of the sequential loading of 17 pL droplets, one microwell can accommodate three droplets, which ultimately merge into one large droplet. During the sequential loading of droplets, the size of the merged droplet will gradually increase. Once the droplet immobilized in the microwell is changed into a plug to block the capillary path located at the exit of the microwell, subsequent droplets are no longer trapped in the microwell but rather move along the bypass channel toward the next empty microwell. We note that the merging of droplets occurs naturally because the concentration of surfactant added in this

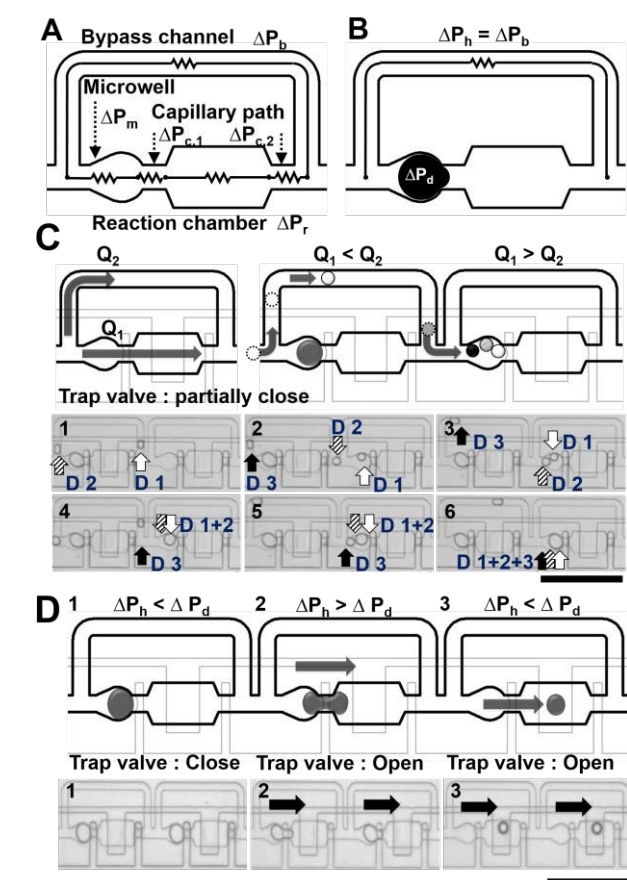


Fig. 2 Principle of handling a droplet in a programmable static droplet array (SDA). (A) Schematic and circuit diagram of a hydrodynamic trap, showing its detailed parts with pressure drops. The microwell, capillary path, and reaction chamber are horizontally connected and the bypass channel is vertically connected to a hydrodynamic trap. (B) Schematic diagram showing the definition of the Laplace and hydraulic pressure drops. A black colored circle indicates a droplet in the microwell, with its Laplace pressure drop. Fluidic resistance in a bypass channel indicates a hydraulic pressure drop. The hydraulic and bypass pressure drops are equal when the microwell is plugged by a droplet. (C) Schematic diagram and time-lapsed images showing the process of droplet arraying. There are two main volumetric flow rates (Q_1 : trapping and Q_2 : bypassing). The black, white and dashed patterned small circles (top) and arrows (bottom) indicate each of the droplets. (D) Schematic diagram and time-lapsed images showing the process of droplet storage. The process of droplet storage can be precisely controlled by the pressure balance of the Laplace (ΔP_d) and hydraulic pressure drops (ΔP_h). The scale bars are (C, D) 400 μm .

experiment is lower than the critical micelle concentration. The droplets are not fully covered with surfactant on their surface and are thus thermodynamically unstable. Thus, the droplets in a microwell tend to thermodynamically stabilize by merging with adjacent droplets.

3.5. Storage

In contrast to previous static droplet microfluidic devices,^{27,29-33} we developed a simple and robust method to dramatically increase the number of droplets stored in a specific position with high combinatorial composition. This method, which we call "storage", allows us to create a single droplet composed of twelve droplets in a single hydrodynamic trap with zero loss. The 12 combinatorial droplets could principally provide 12 factorial designs in a single droplet. The "storage" method, illustrated in Fig. 2D, uses the exact simultaneous opening of a trap valve (also see process 2 in Movie S1, ESI†). The storage process transfers a droplet immobilized in a microwell into the reaction chamber (Fig. 2D). The basic principle of storage is the correlation between the hydraulic pressure drop and the Laplace pressure of the droplet (Fig. 2A and B).

Due to the structure of the channel and its low height (15 μm), the droplet is deformed into a flattened disk. By assuming that there are neither an advancing contact angle nor a receding contact angle in the flow of a continuous phase within a channel, the model of the hydrodynamic trap and the droplets is simplified, and the pressure drop on the inside and outside of the droplets is calculated based on the Laplace principle as follows:

$$\Delta P_d = P_{\text{inside}} - P_{\text{outside}} = \gamma \left(\frac{1}{R_1} + \frac{1}{R_2} \right) \quad (6)$$

ΔP_d indicates the Laplace pressure of the droplet, R_1 the radius in the horizontal direction, R_2 the radius in the vertical direction, and γ the interfacial tension.

The hydraulic pressure drop in the trapping mode (scheme 1 in Fig. 2D) is 0.77 kPa, whereas the Laplace pressure of the droplet is 5.25 kPa, indicating that in the dimensions of our SDA, the Laplace pressure of the droplet is greater, so a droplet can be immobilized in the microwell. Briefly, upon opening the trap valve (scheme 2 in Fig. 2D), the capillary path is opened, and the droplet in the microwell is deformed because the Laplace pressure of the droplet gradually decreases (0.75 kPa). In contrast, the hydraulic pressure drop is maintained at 0.77 kPa and the droplet Laplace pressure decreases further, which indicates that the droplets leave the microwell through the opened capillary path and move toward the reaction chamber.

The mechanism of droplet storing in reaction chamber relies on the Laplace pressure due to the different heights of microchannels.^{39,40} Interestingly, the droplet in the microwell has a flattened disk shape, whereas it looks like a small sphere in the reaction chamber. The apparent volume of the droplet in the reaction chamber looks smaller than that in the microwell due to the different heights of two structures, although there is no change in the volume of the droplet

(scheme 3 in Fig. 2D). The fluctuation valve located at the reaction chamber has a concave bottom due to the negative pressure caused by the higher height of the reaction chamber (30 μm). The difference in the heights of the capillary path (15 μm) and the reaction chamber causes the Laplace pressure of the droplet (0.50 kPa) to be higher than the hydraulic pressure (0.37 kPa) in the reaction chamber. As a result, the droplet can be safely immobilized in the reaction chamber.

3.6 Additional processes

3.6.1. Mixing (Fluctuation)

In the case of (bio) chemical reactions on a small scale, it is occasionally important to increase the mixing efficiency, although diffusion can induce sufficiently homogeneous mixing in the merging of the droplets. However, to our knowledge, there have been few reports of the enhancement of mixing efficiency in droplet microfluidic devices. The SDA device integrated with a fluctuation valve at the reaction chamber for the stable trapping of merged droplets and increasing combinatorial droplets can be used for fluctuation driven by the actuating valve with an alternating change between positive and negative pressures (see process 3 in Movie S1, ESI†). When negative pressure is applied to the fluctuation valve (-0.18 MPa), the valve is expanded downward, which creates a concave-shaped bottom at the reaction chamber. On the other hand, when positive pressure is applied to fluctuation valve (0.18 MPa), the valve is expanded upward, which creates a convex-shaped bottom at the reaction chamber. The cycle of fluctuation is defined as an alternating change of positive and negative pressure, and the frequency is 1 Hz (see Fig. S5†). Interestingly, this fluctuation generates vortex in droplet. If there is no vortex in droplet, mixing in static droplet depends on diffusion of molecules. To clarify the generation of vortex, we demonstrate it with non-motile yeast cells to monitor vortex flow in the droplet (see Fig. S5D†). While actuating fluctuation valve, yeast cells move around and are drifted by irregular vortex in the droplet. Otherwise, irregular vortex flow is not created. Yeast cells in the droplet show random Brownian motion. As shown in Fig. S5E†, we quantitatively analyze the total moving distance of each yeast cell and demonstrate the existence of irregular vortex flow in fluctuated droplet. We expect that this can be used to efficiently decrease the mixing time.

3.6.2. Retrieval

One important characteristic of this SDA is that we are able to retrieve the droplets from the hydrodynamic traps. All of the reaction chambers in the hydrodynamic trap stably contain each droplet in the closed trap valve state. Even when the trap valve is in the opened state, hydrodynamic traps can still stably contain the elastic droplets because the Laplace pressure is still higher than the hydraulic pressure (Fig. 3A, left). However, when we switch on the fluctuation valve with an open state trap valve, the competition between the Laplace pressure and hydraulic pressure is temporarily inverted by the deformation of the fluctuation valve and droplet (Fig. 3A, right). Taking

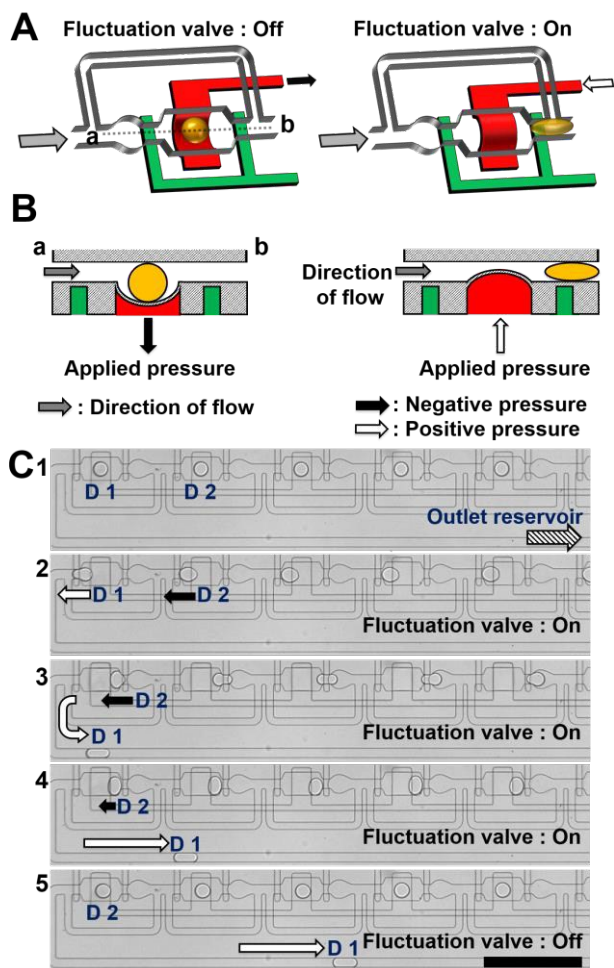


Fig. 3 Schematic diagram of the droplet retrieval process. (A) 3D illustration of the hydrodynamic trap containing an integrated valve. Green and red represent the trap valve and fluctuation valve, respectively. Yellow colored circle and ellipse represent the movement of the droplet. White and black arrows represent the applied negative and positive pressure, respectively. (B) Cross-sectional view of a-b in Fig. 3A during droplet retrieval. (C) Single droplets are sequentially released by simple actuating trap and fluctuation valves.

advantage of this characteristic, we can retrieve a trapped droplet from the reaction chamber by turning the trap valve off and switching the fluctuation valve.

Here, we propose a simple retrieval method that can sequentially release an individual droplet by actuating trap and fluctuation valve. Fig. 3C shows sequential images of the retrieval process with single droplet level (also see process 4 in Movie S1, ESI[†]). When trap valve is switched “off” and fluctuation valve is switched “on”, the droplets in reaction chamber are sequentially released. Then released droplets are re-trapped in front of the subsequent fluctuation valve because the “on” state of fluctuation valve produces a narrow channel as a capillary path in the reaction chamber (Fig. 3C, 1 to 4). And then the fluctuation valve is switched “off” to make a concave-shaped bottom in the reaction chamber. Droplets are temporarily immobilized into reaction chambers again (Fig. 3C, 5). The repeating procedure can release all droplets with single droplet level. Therefore, we will perform off-line or on-

line analysis of analytical apparatus such as mass spectrometry or spectroscopy.

Moreover, our simple retrieval method can achieve a perfectly empty state with no residue or debris in the SDA which enables the strong advantage of reusability, whereas conventional microfluidic systems, including droplet devices, are disposable. Droplets that are not removed disappear within a few seconds. The release rate of the droplets can be improved by increasing the flow rate of the immiscible oil and the frequency of the fluctuation valve application. It will be possible to implement multiple retrieval attempts to significantly increase the success probability in an automated system.

The merits of the reuse of the SDA are to dramatically reduce the preparation time for experiments, the elimination of complicated connection procedures with the reagent solution, sample or reagent waste, and the reduction of the analytical cost. Finally, we can establish a continuous assay system.

3.7. Formation of a combinatorial droplet array

The continually increasing number of chemical compounds poses a unique challenge to develop rapid and efficient methods to screen these libraries. The capability of augmenting the combinatorial content is a critical characteristic necessary for this microfluidic SDA approach to find wide utility. Basically, a combinatorial droplet array means that one droplet can comprise various elements by sequentially repeating the droplet merging, storage, and mixing. The SDA device is designed to trap a droplet of a specific size, and we have successfully manipulated the number of droplets immobilized in a hydrodynamic trap by tuning the size of the droplet. Flexible control of the number of droplets immobilized in a trap produces a highly desirable combinatorial array and results in performance comparable to that of a conventional microwell system due to the fully automated procedure on demand.

Once the droplets are formed in the microwells, they transfer into the reaction chamber, obtaining newly empty microwells. We can repeat the process four times to obtain a single droplet consisting of 12 combinatorial elements. Here, we demonstrate the potential for this device as a tool for screening or combinatorial assays. In this demonstration, three types of solutions, colorless water and green and red fluorescent molecules, are introduced and arrayed (Fig. 4). These droplets represent a physically isolated solution with different chemical entities in an actual combinatorial library method.

Fig. 4 demonstrates the process of forming a combinatorial droplet array with colorless water and green and red fluorescent liquids. To form the first row of the array, three droplets of red, green, and red fluorescent are consecutively immobilized into the first, second, and third microwells, respectively. Then, we perform a storage process to transfer the droplets in the microwells into the reaction chambers. As a result of the storage process, the SDA rapidly regains its empty

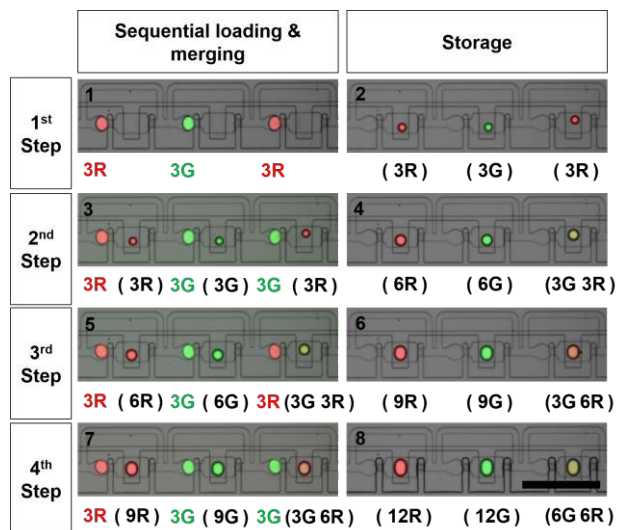


Fig. 4 Formation of the combinatorial droplet array. Overlaid fluorescence and bright field images show the generation of a multiple-droplet array in three hydrodynamic traps. A combinatorial droplet array is generated by repeating the sequential loading, merging and storage process. Red and green fluorescent dyes are used to represent the chemically distinct compositions of the droplet. In the sequential loading and merging steps, triple droplets are trapped in each microwell. In the storage steps, the trapped droplets are stored in the corresponding reaction chambers. Previously stored droplets do not significantly affect the next array process until the reaction chamber is fully occupied (220 pL). After the fourth storage step, the stored droplet is composed of twelve small droplets with twelve compositions. The compositions of the stored droplets are programmed and formulated by the sequence of generated droplets. Scale bar, 400 μm .

microwells. The whole process of sequential loading, merging, and storage can repeat four times because the reaction chamber can accommodate a 220 pL droplet. As a proof of concept, we present several different fluorescence colors and intensities in each droplet. If the volume of the droplet in the reaction chamber exceeds 220 pL, the fluid flowing horizontally is blocked, and thus it is no longer possible to array and store droplets. Hence, the SDA could involve only four steps. In each step, three droplets are stored in the reaction chamber of a hydrodynamic trap, and thus single droplet stored in the reaction chamber comprises 12 individual droplets in total. The user can therefore manipulate the composition of a single droplet with 12 factorial cases, corresponding to the actual demand of the combinatorial library. The result proves that the SDA would be useful for high content screening.

To demonstrate the controllability of a more complicated arbitrary and addressable formulation, we apply the SDA device as a programmable display (Fig. 5). The displayed letters represents the initials of 'Chungnam National University.' The letter 'C' shows a linear gradient of red fluorescence from the upper to the bottom line, which is formed by dispensing programmed numbers of droplets of 1 μM dye and water. The letter 'N' shows a linear gradient of green fluorescence from the upper to the bottom line, which is formed by dispensing programmed numbers of droplets of 100 μM dye and water. The letter 'U' forms a reverse gradient of red (downward) and green fluorescence (upward). A quantitative analysis of the

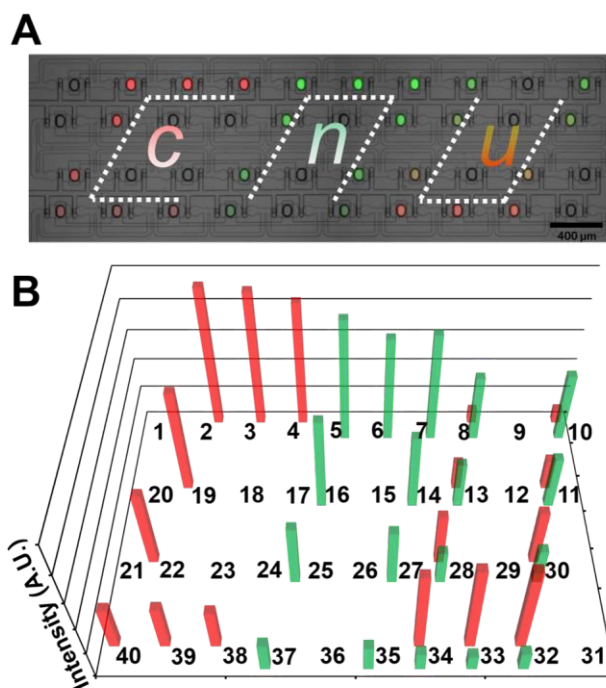


Fig. 5 Demonstration of arbitrary and addressable formulation of droplets in an SDA device. (A) Overlaid fluorescent and bright field microscope images showing the microfluidic display in the 40 hydrodynamic traps using red and green fluorescent dyes and water to display letters. The letter 'c' is produced using red fluorescent dye and water to generate a concentration gradient of red fluorescent dye. The letter 'n' is generated using a concentration gradient of green fluorescent dye. The letter 'u' is a gradient of green and red fluorescent dyes. The transparent droplets are composed of only water. (B) Corresponding normalized intensities for the microfluidic display. The number is the index of the droplet array in Fig. 5A. No cross-contamination of fluorescent molecules could be observed. We note that the overlaid image of red and green fluorescent images would display as yellowish. Scale bar indicates 400 μm .

CNU display in the fluorescence and intensity shows corresponding values on demand. The result proves that the programmable SDA has excellent programmability without cross-contamination.

3.8. Enzymatic reactions in droplets and reuse

3.8.1. Enzymatic reactions

Our SDA can perform a one-pot analysis using array of equivalent droplets that serve as identical experimental units with a specific composition. As a demonstration, we analyzed an enzymatic reaction between β -galactosidase (β -gal) and fluorescein di(β -D-galactopyranoside) (FDG) (Fig. 6A). The enzyme β -gal can cleave off the fluorescein molecule on the FDG substrate by hydrolysis. With the SDA device, we prepared an accurate number of droplets of the four aqueous reagents, including β -gal, FDG, PBS buffer, and water. Each reagent is individually loaded into the corresponding reagent channels. FC-40 oil is used as a continuous fluid that contains 30 v/v% of 1H, 1H, 2H, 2H-perfluoro-1-octanol.

We performed a one-pot analysis with 40 droplet reactors in a single SDA device, with 10 identical enzyme reactions with 4 specific concentrations (each row: FDG concentrations of 0, 3.3, 6.6, 10 μM , respectively) (Fig. 6B). First, the concentration

ARTICLE

Journal Name

of FDG for each row as precisely controlled by the combinatorial sequences of sequential loading, merging and storage of the FDG and PBS buffer droplets (final droplet reactor volume: 153 μL). Next, we delivered 51 μL droplets containing 50 units/mL of enzyme β -gal into each microwell. Then, the storage and mixing of the droplets initiated the hydrolysis of FDG by β -gal, producing a fluorescence signal. Using these processes, the 40 individual enzymatic reactions initiated simultaneously in each reaction chamber. The enzymatic activity of β -gal can subsequently be measured by monitoring the development of the fluorescent intensity with time. Fig. 6B shows the increased normalized fluorescent intensity versus time in the range of 10, 6.6, 3.3, and 0 μM of FDG. Each point of data and standard deviation were presented as the average values in the ten droplets. Moreover, 10 identical enzyme reactions with 4 specific concentrations were just performed in a one-pot analysis and these reactions were completed within just 25 seconds in our SDA. This indicates that our SDA is suitable for monitoring a fast reaction that scales within a few seconds.

As we demonstrated, our SDA is an efficient platform for biological assays that quantitatively monitor a series of kinetic reactions of varying compositions. It would contribute to the screening of libraries by reducing the costs of time, labor and reagents because a one-pot analysis is available with a single device.

3.8.2. Reuse experiment

Our current SDA device has 40 hydrodynamic traps for completing an individual reaction. For biochemical screening, though, this might not be sufficient to monitor the libraries. To overcome this issue, we reuse the SDA device to enhance the throughput. The reuse of the SDA to dramatically reduce the preparation time for each experiment establishes a continuous assay system.

We tested the reusability of our SDA device (Fig. 6C). We measured the success rate of the enzymatic assay in one reused device, with the same experiments repeated in three devices, and a 100% success rate was achieved until the 27th reaction (Fig. 6C). We attribute this to residual protein absorption in the hydrophobic PDMS, although 27 cycles is quite substantial compared to other single-use disposable devices. Residual proteins can also cause spreading and deformation of the droplets when reusing the SDA several times. To enhance the reusability of our SDA device, we focus on the properties of PDMS, which can be easily cleaned and reused several times. When the assay is finished, all of the droplets are eliminated by a retrieval process, and the empty channel is washed by flushing the water plug. Although the residual proteins are adsorbed in the channel, a study of the probability of droplet array formation after several cycles of enzymatic reactions reveals a high success rate of perfect arraying without any misarraying over short intervals. Clearly, the result indicates that the SDA is useful, more efficient than conventional disposable microfluidic devices, and enables a dramatic reduction of cost. The high probability of reuse is attributed to the ease of formation of the droplet array and its

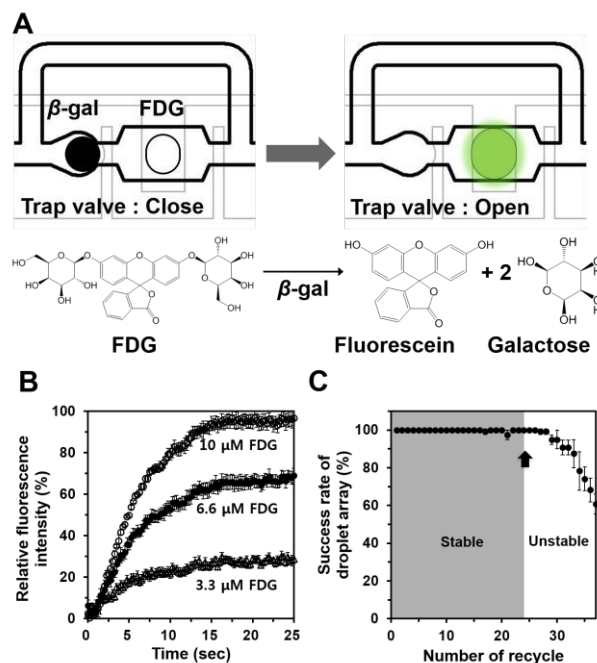


Fig. 6 One-pot analysis of enzyme reaction in an SDA device and reusability of the device. (A) Schematic diagram of enzyme assay in the SDA device. Fluorescein di(β -D-galactopyranoside) (FDG) contains a fluorescent product with two galactose units. β -galactosidase (β -gal) is a hydrolase enzyme that cleaves off the fluorescein molecule from the FDG substrate. A concentrated FDG droplet is prepared by repeating three cycles of sequential loading and storage. Afterwards, we introduce a β -gal droplet to initiate the enzyme reaction. (B) Time versus enzymatic assay curve. A one-pot analysis is performed in a single experiment of SDA with 10 identical enzyme reactions with 4 specific concentrations (0, 3.3, 6.6, 10 μM). The entire reaction is finished in 25 seconds, and the error bars represent the standard deviations in 10 droplets. (C) Success rate of enzymatic assay in a recycled SDA device. Three devices are used in this experiment. In all cases, a 100% success rate is obtained until the 27th reaction. Error bars represent the standard deviations in the three devices.

perfect removal because the design of the SDA integrated with a microvalve system and automatic control increases the system's stability and overcomes conventional technical huddles.

4. Conclusions

Here, we developed a programmable microfluidic SDA device that could perform multipurpose experiments for various users. It operates several processes to precisely control the composition of the droplet array. First, it can generate a droplet on demand with a specific volume, generation order of droplets, and gap between adjacent droplets. Second, it exhibits the principle of passive hydrodynamic trapping without additional control necessary to array the droplets in a predefined region. Third, the process of droplet storage can increase the numbers of droplets that produce the desired composition. Fourth, the combinatorial formation of an array could be controlled as desired. Finally, the SDA can be reused to conduct a number of independent experiments with perfect addressability, no waste, and green chemistry. These processes are programmable and automatically operated,

which can allow a user to easily utilize our SDA device for their own purpose.

Compared with a conventional microtiter plate system, our microfluidic SDA offers a promising alternative because it requires only minute amounts of reagents and allows the continuous observation of a reaction throughout the screening. Additionally, it has the general benefit of microfluidics that allows the possibility of generating a wide spectrum of concentrations from small volumes of reagents for screening purposes, which is challenging for other methods. Moreover, our proposed device has advantages even for applications that do not require post-analyses, such as chemical detection and clinical diagnostic purposes, in which the identities of the probes are known in advance. After the test, all of the droplets can be removed and replaced for another round of screening. Such a flexible and reusable format will greatly reduce the cost of droplet-based assays.

Acknowledgements

This study was supported by a grant from the National Research Foundation of Korea (NRF), funded by the Korean government (MEST) (No. 2011-0017322).

References

- 1 S. L. Anna, N. Bontoux and H. A. Stone, *Appl. Phys. Lett.*, 2003, **82**, 364.
- 2 S. Takeuchi, P. Garstecki, D. B. Weibel and G. M. Whitesides, *Adv. Mater.*, 2005, **17**, 1067-1072.
- 3 A. S. Utada, E. Lorenceau, D. R. Link, P. D. Kaplan, H. A. Stone and D. A. Weitz, *Science*, 2005, **308**, 537-541.
- 4 S. Y. Teh, R. Lin, L. H. Hung and A. P. Lee, *Lab Chip*, 2008, **8**, 198-220.
- 5 C. H. Choi, D. A. Weitz and C. S. Lee, *Adv. Mater.*, 2013, **25**, 2536-2541.
- 6 J.-O. Nam, C.-H. Choi, J. Kim, S.-M. Kang and C.-S. Lee, *Korean Chem. Eng. Res.*, 2013, **51**, 597-601.
- 7 Y. Song and C.-S. Lee, *Korean Chem. Eng. Res.*, 2014, **52**, 632-637.
- 8 Y.-R. Lee, J. Kim and W.-S. Ahn, *Korean J. Chem. Eng.*, 2013, **30**, 1667-1680.
- 9 R. S. Boogar, R. Gheshlaghi and M. A. Mahdavi, *Korean J. Chem. Eng.*, 2013, **30**, 45-49.
- 10 C. H. Choi, J. Kim, J. O. Nam, S. M. Kang, S. G. Jeong and C. S. Lee, *ChemPhysChem*, 2014, **15**, 21-29.
- 11 H.-H. Jeong, Y.-M. Noh, S.-C. Jang and C.-S. Lee, *Korean Chem. Eng. Res.*, 2014, **52**, 141-153.
- 12 A. R. Abate, M. B. Romanowsky, J. J. Agresti and D. A. Weitz, *Appl. Phys. Lett.*, 2009, **94**, 023503.
- 13 F. Guo, K. Liu, X.-H. Ji, H.-J. Ding, M. Zhang, Q. Zeng, W. Liu, S.-S. Guo and X.-Z. Zhao, *Appl. Phys. Lett.*, 2010, **97**, 233701.
- 14 S. H. Jin, J. Kim, S.-C. Jang, Y. M. Noh and C.-S. Lee, *Korean Chem. Eng. Res.*, 2014, **52**, 106-112.
- 15 M. G. Pollack, A. D. Shenderov and R. B. Fair, *Lab Chip*, 2002, **2**, 96-101.
- 16 L. Wang, L. A. Flanagan, E. Monuki, N. L. Jeon and A. P. Lee, *Lab Chip*, 2007, **7**, 1114-1120.
- 17 Y. Li, C. Dalton, H. J. Crabtree, G. Nilsson and K. V. Kaler, *Lab Chip*, 2007, **7**, 239-248.
- 18 S. K. Cho, Y. Zhao and C. J. Kim, *Lab Chip*, 2007, **7**, 490-498.
- 19 S. Koster, F. E. Angile, H. Duan, J. J. Agresti, A. Wintner, C. Schmitz, A. C. Rowat, C. A. Merten, D. Pisignano, A. D. Griffiths and D. A. Weitz, *Lab Chip*, 2008, **8**, 1110-1115.
- 20 J. J. Agresti, E. Antipov, A. R. Abate, K. Ahn, A. C. Rowat, J. C. Baret, M. Marquez, A. M. Klibanov, A. D. Griffiths and D. A. Weitz, *Proc. Natl. Acad. Sci. U. S. A.*, 2010, **107**, 4004-4009.
- 21 C. H. Chen, A. Sarkar, Y. A. Song, M. A. Miller, S. J. Kim, L. G. Griffith, D. A. Lauffenburger and J. Han, *J. Am. Chem. Soc.*, 2011, **133**, 10368-10371.
- 22 A. Fallah-Araghi, J. C. Baret, M. Ryckelynck and A. D. Griffiths, *Lab Chip*, 2012, **12**, 882-891.
- 23 S. S. Lee, I. Avalos Vizcarra, D. H. E. W. Huberts, L. P. Lee and M. Heinemann, *Proc. Natl. Acad. Sci. U. S. A.*, 2012, **109**, 4916-4920.
- 24 S. Cho, D. K. Kang, S. Sim, F. Geier, J. Y. Kim, X. Niu, J. B. Edler, S. I. Chang, R. C. Wootton, K. S. Elvira and A. J. deMello, *Anal. Chem.*, 2013, **85**, 8866-8872.
- 25 K. Leung, H. Zahn, T. Leaver, K. M. Konwar, N. W. Hanson, A. P. Page, C. C. Lo, P. S. Chain, S. J. Hallam and C. L. Hansen, *Proc. Natl. Acad. Sci. U. S. A.*, 2012, **109**, 7665-7670.
- 26 W. H. Tan and S. Takeuchi, *Proc. Natl. Acad. Sci. U. S. A.*, 2007, **104**, 1146-1151.
- 27 W. Shi, J. Qin, N. Ye and B. Lin, *Lab Chip*, 2008, **8**, 1432-1435.
- 28 T. Teshima, H. Ishihara, K. Iwai, A. Adachi and S. Takeuchi, *Lab Chip*, 2010, **10**, 2443-2448.
- 29 M. Sun, S. S. Bithi and S. A. Vanapalli, *Lab Chip*, 2011, **11**, 3949-3952.
- 30 H. H. Jeong, S. H. Jin, B. J. Lee, T. Kim and C. S. Lee, *Lab Chip*, 2015, **15**, 889-899.
- 31 S. S. Bithi and S. A. Vanapalli, *Biomicrofluidics*, 2010, **4**, 44110.
- 32 A. Dewan, J. Kim, R. H. McLean, S. A. Vanapalli and M. N. Karim, *Biotechnol. Bioeng.*, 2012, **109**, 2987-2996.
- 33 S. S. Bithi, W. S. Wang, M. Sun, J. Blawdziewicz and S. A. Vanapalli, *Biomicrofluidics*, 2014, **8**, 034118.
- 34 M. A. Unger, H.-P. Chou, T. Thorsen, A. Scherer and S. R. Quake, *Science*, 2000, **288**, 113-116.
- 35 C. C. Lee, G. D. Sui, A. Elizarov, C. Y. J. Shu, Y. S. Shin, A. N. Dooley, J. Huang, A. Daridon, P. Wyatt, D. Stout, H. C. Kolb, O. N. Witte, N. Satyamurthy, J. R. Heath, M. E. Phelps, S. R. Quake and H. R. Tseng, *Science*, 2005, **310**, 1793-1796.
- 36 S. Zeng, B. Li, X. Su, J. Qin and B. Lin, *Lab Chip*, 2009, **9**, 1340-1343.
- 37 W. S. Lee, S. Jambovane, D. Kim and J. W. Hong, *Microfluid. Nanofluid.*, 2009, **7**, 431-438.
- 38 H. Zec, T. D. Rane and T. H. Wang, *Lab Chip*, 2012, **12**, 3055-3062.
- 39 P. Abbyad, R. Dangla, A. Alexandrou and C. N. Baroud, *Lab Chip*, 2011, **11**, 813-821.
- 40 E. Fradet, C. McDougall, P. Abbyad, R. Dangla, D. McGloin and C. N. Baroud, *Lab Chip*, 2011, **11**, 4228-4234.